Behavioral/Systems/Cognitive

Distinct Signals Conveyed by Pheromone Concentrations to the Mouse Vomeronasal Organ

Jie He,[1] Limei Ma,[1] Sangseong Kim,[1] Joel Schwartz,[1] Michael Santilli,[1] Christopher Wood,[1] Michael H. Durnin,[1] and C. Ron Yu[1,2]

[1]Stowers Institute for Medical Research, Kansas City, Missouri 64110, and [2]Department of Anatomy and Cell Biology, University of Kansas Medical Center, Kansas City, Kansas 66160

In mammalian species, detection of pheromone cues by the vomeronasal organ (VNO) at different concentrations can elicit distinct behavioral responses and endocrine changes. It is not well understood how concentration-dependent activation of the VNO impacts innate behaviors. In this study, we find that, when mice investigate the urogenital areas of a conspecific animal, the urinary pheromones can reach the VNO at a concentration of ~1% of that in urine. At this level, urinary pheromones elicit responses from a subset of cells that are tuned to sex-specific cues and provide unambiguous identification of the sex and strain of animals. In contrast, low concentrations of urine do not activate these cells. Strikingly, we find a population of neurons that is only activated by low concentrations of urine. The properties of these neurons are not found in neurons responding to putative single-compound pheromones. Additional analyses show that these neurons are masked by high-concentration pheromones. Thus, an antagonistic interaction in natural pheromones results in the activation of distinct populations of cells at different concentrations. The differential activation is likely to trigger different downstream circuitry and underlies the concentration-dependent pheromone perception.

Introduction

In terrestrial animals, pheromones play an important role in intra-species communication, eliciting a range of innate and often stereotyped behaviors (Birch, 1974; Wyatt, 2003). Animals have evolved various means, such as urine marking, fecal deposition, and flank marking, to broadcast pheromone signals (Ralls, 1971; Humphries et al., 1999; Rich and Hurst, 1999; Hurst and Beynon, 2004). The deposited pheromones can have long-lasting effects, especially for the less volatile compounds produced in the vertebrate species (Wyatt, 2003). Moreover, vertebrate animals have evolved strategies to deposit pheromones with carriers, such as the lipacalin family of proteins, to slow down the fading of signals (Keverne, 1998; Beynon and Hurst, 2003). Because pheromones from different individuals are deposited at various times, the concentration and the context in which these signals are detected vary by a large degree and have strong influences on innate behaviors (Bronson, 1979; Kaba et al., 1989; Johnston, 1998; Brennan and Kendrick, 2006). In territorial marking behaviors, for example, high and low concentrations of urinary pheromones have diametric effects (Beauchamp et al., 1982; Nevison et al., 2003; Hurst and Beynon, 2004). Male mice usually avoid fresh, high-concentration urine marks of other males, whereas stale or low-concentration urine elicits strong countermarking behaviors (Humphries et al., 1999). Conversely, high doses of pheromones are generally required to trigger endocrine changes. For example, Drickamer and colleagues reported a dose-dependent delay of estrus onset by urine from group-housed female mice (Drickamer, 1982). Similarly, direct contact with male urine is significantly more potent than soiled bedding in accelerating estrus onset (Drickamer and Assmann, 1981; Drickamer, 1986).

It is not understood how pheromone at different concentrations affects innate behaviors. One possibility is that a high concentration of pheromones activates more neurons to reach the threshold of behavioral output. In the main olfaction system, increasing odor concentrations leads to the activation of larger numbers of sensory neurons and more glomeruli in the olfactory bulb (Mori et al., 1999; Rubin and Katz, 1999; Meister and Bonhoeffer, 2001). However, it is not clear whether the vomeronasal organ (VNO) neurons respond similarly. It has been reported that the pheromone activation of the VNO neurons is highly specific, and these neurons are not activated by additional ligands even at high concentrations (Leinders-Zufall et al., 2000). Alternatively, synergistic and antagonistic interactions among pheromone components with their receptors could produce complex response patterns such that distinct sets of neurons are activated at different concentrations. The VNO expresses ~250 G-protein-coupled, seven-transmembrane receptors (Dulac and Axel, 1995; Herrada and Dulac, 1997; Matsunami and Buck,

Received Feb. 15, 2010; revised March 26, 2010; accepted April 16, 2010.

This work is supported by funding from Stowers Institute and National Institutes of Health/National Institute on Deafness and Other Communication Disorders Grant 008003 (C.R.Y.). U.S. patent pending (U.S. Patent Application No. 60/863,301, pending) for the tetO-G-CaMP2 mice (Stowers Institute, C.R.Y., L.M.). We thank Drs. W. Wiegraebe and D. Zhu for help on imaging and statistical analyses. We thank E. Gillespie, P. Zelalem, Megan Fracol, G. Hattem, M. Elmore, S. Klinefelter, K. Cavanaugh, and Lab Animal Service Facility and Microscopy Center at Stowers Institute for technical assistance. The ESP-1 plasmid was generously provided by Dr. K. Touhara (University of Tokyo, Tokyo, Japan). We also thank Drs. M. Gibson, R. Krumlauf, H. Y. Mak, and K. Si for thoughtful discussions and critical reading of this manuscript.

Correspondence should be addressed to C. Ron Yu, Stowers Institute for Medical Research, 1000 East 50th Street, Kansas City, MO 64110. E-mail: cry@stowers.org.

J. Schwartz's present address: Duke University Medical Center, Box 3209, Bryan Research Building, Research Drive, Durham, NC 27710.

DOI:10.1523/JNEUROSCI.0825-10.2010

 0270-6474/10/307473-11$15.00/0

1997; Ryba and Tirindelli, 1997; Pantages and Dulac, 2000; Zhang et al., 2004; Yang et al., 2005). Each vomeronasal neuron expresses only one specific type of these receptors. Projections from neurons expressing the same receptor converge to the accessory olfactory bulb in a stereotyped manner (Belluscio et al., 1999; Rodriguez et al., 1999; Del Punta et al., 2002; Wagner et al., 2006). Thus, the differential activation of VNO neurons is likely to trigger neural circuitries that lead to distinct behavioral outputs. In this study, we measured the effective concentration of pheromones reaching the VNO and examined concentration-dependent activation of the VNO.

Materials and Methods

Animals. The generation of the tetO–G-CaMP2 mice was described previously (He et al., 2008). These mice were crossed to the OMP–IRES–tTA line (Yu et al., 2004) to restrict expression of G-CaMP2 in the olfactory sensory neurons (OSNs). Pheromone-evoked responses were obtained from a total of 24 2- to 6-month-old mice (13 males and 11 females). Dye labeling experiments were performed using a total of 12 animals of the C57BL/6J strain. Animals were maintained in the Lab Animal Services Facility of Stowers Institute at 12 h light/dark cycle and were provided with food and water *ad libitum*. Experimental protocols were approved by the Institutional Animal Care and Use Committee at Stowers Institute and were in compliance with the National Institutes of Health *Guide for Care and Use of Animals*.

Electro-vomeronasogram recording. In electro-vomeronasogram (EVG) experiments, local field potentials were recorded from the microvillous layer of intact VNO sensory epithelia as described previously (Leinders-Zufall et al., 2000; Leypold et al., 2002). Briefly, the VNO epithelium was exposed and perfused with oxygenated mouse artificial CSF (mACSF). Field potential was recorded using glass pipettes (10 μm diameter) connected to an AI 401 preamplifier (Molecular Devices). The signals were further amplified by a signal conditioner (Molecular Devices), digitized at 1 kHz, and low-pass filtered at 20 Hz. The data was further analyzed using Clampfit 10.0 (Molecular Devices). Urine samples at dilutions specified in the text were delivered through another glass pipette (10 μm diameter). Urine samples were delivered to the recording sites by a 1 s pulse of air pressure controlled by Pressure System 2 (Toohey Company). Phenol red at 0.1% was added to all urine and control solutions such that the pulse of application could be visualized. The constant overflow of oxygenated mACSF quickly removed the urine application away from the VNO surface, as visualized from the dispersion of phenol red. Occasionally, pressure delivery of urine induced mechanical artifacts. The artifacts were characterized by the abrupt changes in electrical signals timed to the onset and offset of the application. The mechanical artifacts were readily distinguishable from urine-induced responses, which were characterized by significantly slower and smoother time courses. Records with artifacts were excluded from additional analyses. Each recording was obtained from a single site with a single application of urine. Recordings were performed with seven mice with four to seven recording sites used from each VNO preparation. Recordings were first made from a site downstream of the superfused mACSF and moved upward, ending with the most upstream site. This order of recordings precluded potential inactivation or desensitization of neurons that might result from multiple exposures. Traces shown in Figure 1 were those with amplitude close to the mean as shown in *D*. The composition of mACSF is as follows (in mM): 130 NaCl, 5 KCl, 1 $MgCl_2$, 2.5 $CaCl_2$, 1.25 NaH_2PO_4, 25 $NaHCO_3$, and 10 glucose.

Dye labeling of the VNO. Fresh urine was collected and used to dissolve Rhodamine 6G (Sigma) to 100 μM. The dye-containing urine was then painted onto the urogenital area of anesthetized female mice. C57BL/6J male mice were then introduced to the cages containing the painted mice one at a time. The investigation of the females by the males was monitored to count the number of investigations. A bout of investigation is defined as a period in which the male continuously poked and pushed into the urogenital area of the female. Disengagement from the area was considered as the end of a bout. After either a single bout or three bouts of investigation, the male animals were killed, and the VNOs were dissected out for confocal imaging. After each individual VNO was taken out from the nasal cavity, the lateral vomer bone encasing the VNO was removed. The blood vessel covering the neuroepithelia was lifted to expose the dendritic surface of the sensory epithelium. The lumenal surface was imaged using the Carl Zeiss LSM 510 confocal system mounted on a Carl Zeiss AxioScope2 FS microscope. A 5× air lens (numerical aperture 0.15) was used to perform the imaging. The samples were excited using a 514 nm wavelength argon laser, and the emission light was detected by a Meta detector set between 544 and 576 nm wavelength. Pinhole size was set at 82 μm. *Z*-series of optical sections were obtained at 10 μm steps. For each region of interest (ROI), signals measured at different *z*-depth were plotted. The peak amplitude of the signals was used to estimate the dye concentration within the region of interest. Under the same optical condition, Rhodamine 6G solutions at 0, 0.1, 0.5, and 1 μM concentrations were measured. A standard curve based on the free dye measurement was extrapolated and used to estimate dye concentrations in the VNO. Similar procedures were performed for sulforhodamine 101 and rhodamine-conjugated dextran.

To estimate the thickness of the mucus layer, signals from the *z*-series measurement for each ROI were deconvolved from the *z*-axis point spread function of the confocal scope, assuming a Gaussian distribution along *z*. The optical section thickness was determined by the pinhole size and equaled 50 μm in these imaging experiments. The deconvolved signals were then fitted with a Gaussian curve, and the full-width at half-maximum (FWHM) of the fitted curve was used to estimate the thickness of the lumenal mucus.

Pheromones and chemicals. Urine samples were collected from animals using the free-catch method. The freshly collected urine samples were frozen at −80°C until use for up to 3 months. After thawing the samples, the tubes were spun for 1 min to collect the condensations and reduce the loss of substances. All other chemicals were obtained from Sigma-Aldrich. Recombinant ESP-1 was prepared from a plasmid provided by Dr. K. Touhara (University of Tokyo, Tokyo, Japan) as described by Kimoto et al. (2005).

VNO slice preparation. Two- to 6-month-old mice of both sexes were decapitated after death by CO_2 inhalation. The VNO was removed from the bone capsule and embedded in 4% low melting agarose. Coronal slices (200 μm) were prepared in oxygenated mACS at 4°C using Vibratome 3000 sectioning system. Slices were kept in oxygenated (95%O_2/5%CO_2) mACSF at room temperature for up to 8 h.

Calcium imaging. Imaging of VNO slices was performed as described previously (He et al., 2008). VNO slices were continuously perfused with oxygenated mACSF at room temperature at a speed of ~1 ml/min. The flow was unidirectional resulting from the placement of the inlet and outlet at opposite ends of the slices. The VNO slices were placed such that the dendrites face the incoming stream. Urine was delivered at various dilutions via BSP-8PG systems using 8, 12, or 16-channel micromanifolds (ALA Scientific). To minimize mechanical artifacts, a continuous flow of Ringer's solution (in mM: 115 NaCl, 5 KCl, 2 $CaCl_2$, 2 $MgCl_2$, 25 $NaHCO_3$, and 5 HEPES) was maintained during the experiment. Flow speed was controlled at 2–3 μl/s. Delivery of urine was achieved by the simultaneous opening of a urine valve and the closing of the Ringer's solution valve to minimize the change in pressure within the manifold and avoid introducing mechanical disturbance to the slices.

Time-lapse recordings of fluorescent signals from the VNO were performed on the Carl Zeiss AxioSkope FS2 microscope with a 10× water-dipping lens (0.3 numerical aperture; 3.3 mm working distance). An EXFO X-Cite 120PC light source equipped with a bandpass filter (450–490 nm) was used to excite the samples. The epifluorescent images were acquired by a CCD camera (Carl Zeiss HRM) with 2 × 2 or 4 × 4 binning depending on the expression levels of G-CaMP2 signal. Most of the data reported here derived from a mouse line designated as 12J, which stably expresses G-CaMP2 in ~50% of the neurons. The same line has been used in our previous publication (He et al., 2008). At the end of some

experiments, confocal images were taken to ensure that no cells overlapped in the ROIs. For most experiments, repetitive applications and reverse-order applications were performed to examine reproducibility of the responses. To ensure the health of the cells and to reduce potential discrepancies introduced by photo-bleaching, individual slices were recorded for no more than 60 min, or 15 recording sessions, each 1 min long. Except for experiments testing urine-induced inactivation, a one 5-min interval was introduced between any pairs of stimuli.

Loose patch recordings. Glass electrode (1.2 mm outer diameter, 0.9 mm inner diameter) was fabricated and polished to have resistance ranging from 3 to 7 MΩ with P-2000 micropipette puller (Sutter Instruments). Extracellular recordings were performed after forming ~100 MΩ seals onto visually identified cells. The pipette solution contained Ringer's solution. Signals were amplified and recorded with MultiClamp 700A amplifier and digitized with Digidata 1440A (Molecular Devices). Spontaneous action potentials and resting membrane potentials were measured under current-clamp mode ($I = 0$) with 10 kHz sampling rate and filtered at 0.5 kHz. Data were acquired and analyzed with Clampex 10.1 and Clampfit 10.1 software (Molecular Devices).

Data analysis. Image processing and data analyses were performed using NIH ImageJ version 1.42 software (http://rsb.info.nih.gov/ij/) as described previously (He et al., 2008). Briefly, a background image sequence was generated by applying Gaussian filter (radius of 50 pixels) from the raw image sequence. A scattering-corrected image was obtained by subtracting the background from the raw image sequence. Subsequently, the scattering-corrected image sequence was divided into pre-pheromone and post-pheromone application substacks. Responding cells emerged from the background after subtracting the preapplication from the postapplication stack. To obtain information on response amplitude and dynamics, individual responsive cells were identified manually using the Multi-Measure Plug-In in NIH ImageJ. Response curves were plotted as $\Delta F/F$. To minimize the signals introduced by the autofluorescence of urine and light scattering from the responsive cells, randomly selected ROIs that were not neighboring any obviously responsive cell were used to calculate overall background changes.

The response heat maps were produced using a custom-written program in either Matlab (MathWorks) or Bioconductor R package (http://www.R-project.org). The maps were based on the value according to the $\Delta F/F$ of each individual response. Cells responding only to a single urine application were not included in the plot.

To perform principal component analysis and cluster analysis, a response matrix was first generated by assigning 1 to cells with $\Delta F/F \geq 0.1$ and 0 to cells with $\Delta F/F < 0.1$. For hierarchical clustering, the R *hclust()* function was applied to the response matrix to group the samples. Pairwise Pearson's correlation values were calculated between samples, and the distance was defined as 1 correlation. The similarity between different samples was plotted as a dendrogram, which grew heuristically by merging pairs of most similar samples into clusters.

Results

Concentration range of natural pheromones detected by the mouse VNO

The VNO is encapsulated in a semiblind bony structure with one opening connected to the nasal cavity (Wysocki and Lepri, 1991; Keverne, 2002). An active pumping mechanism is required to bring pheromones into the lumen of the VNO (Meredith and O'Connell, 1979; Meredith et al., 1980; Pankevich et al., 2003). The unique mechanism by which pheromones are brought into the VNO, as well as the nonvolatile nature of some pheromones, make it difficult to infer the amount of pheromones reaching the VNO directly from their sources.

To estimate the concentration of urine that reached the VNO lumen during free-moving investigation, we painted the urogenital areas of anesthetized animals with mouse urine mixed with different concentrations of a water-soluble dye, Rhodamine 6G. Rhodamine 6G is a polar molecule with a molecular weight of 479.02. These properties are similar to what have been characterized for several putative mouse pheromones in the small-molecular-weight class and are similar to that of small peptides (Novotny et al., 1984, 1985, 1990, 1999; Jemiolo et al., 1986, 1989; Price and Vandenbergh, 1992; Beynon and Hurst, 2003; Nevison et al., 2003). This dye has been used to study the access of nonvolatile compounds to the VNO and the main olfactory epithelium (Wysocki et al., 1980; Leinders-Zufall et al., 2004; Spehr et al., 2006). We reasoned that Rhodamine 6G would allow us to estimate the amount of pheromone entering the VNO in a semiquantitative way, although it might not fully recapitulate the concentration of various pheromones in urine being carried to the VNO.

When male mice were allowed to investigate the painted subjects, fluorescent signals from the dye molecules were observed in their VNOs (Fig. 1*B*). To quantify the amount of dye reaching the VNO, we used laser-scanning confocal microscopy to measure the levels of fluorescence in the VNO. We conducted *z*-series measurement of fluorescent signals in several randomly selected areas. The signal traces for different regions displayed peak values at different depths (supplemental Fig. 1, available at www.jneurosci.org as supplemental material). By comparing the peak fluorescent intensities of various regions with a series of standard dilutions of the dye, we found that dye concentration inside the VNO lumen reached ~0.5 and ~1.5% of that in urine for the one- and three-bout investigations, respectively (Fig. 1*B*,*C*). The relative concentration reaching the VNO increased with repeated investigation; three-bout investigations resulted in approximately threefold increases in the amount of dye reaching the VNO (Fig. 1*C*). We also obtained similar results using a different dye, sulforhodamine 101 (molecular weight of 606.71), in both one-bout and three-bout experiments (supplemental Fig. 2, available at www.jneurosci.org as supplemental material). Interestingly, a higher-molecular-weight conjugate, rhodamine dextran (molecular weight of 10,000), was less effective in entering the VNO and reached 0.2% of the dye level in urine in a three-bout investigation (supplemental Fig. 2, available at www.jneurosci.org as supplemental material). This was ~10 times less than the lower-molecular-weight dyes and suggested that diffusion could play an important role for the pheromones to reach the VNO.

Based on the *z*-series measurement of the fluorescent signals, we also estimated the depths of VNO mucus. By deconvolving image signals from the *z*-axis point spread function of the confocal scope, we obtained an average of 65.14 ± 22.92 μm (mean ± SD) FWHM value for all the regions measured (supplemental Fig. 3, available at www.jneurosci.org as supplemental material). This number provided an estimate of the mucus thickness.

We next tested the detection limit of natural pheromones by the VNO. We addressed this issue by conducting EVG field potential recordings, from the microvillus surface of the VNO. At 10^{-6} urine dilution, the variance of the response was comparable with the amplitude, suggesting that the detection threshold was around this concentration (Fig. 1*D*,*E*). Stepwise increase in urine concentration up to 10^{-2} dilution resulted in increases in EVG amplitude. Together, these data indicated that the mouse VNO could detect natural pheromones varying in concentration of at least four orders of magnitude, from 10^{-6} dilution to a few percentages of whole urine.

Patterns of activation by urine at different concentrations

In the next set of experiments, we examined dose-dependent activation of the VNO at the single-cell level. We conducted calcium imaging experiments from a large population of neurons in VNO slices prepared from transgenic mice expressing the calcium sensor G-CaMP2 in the vomeronasal neurons (He et al., 2008). Pheromones activate the vomeronasal neurons through the activation of their receptors and elicit an increase in intracellular calcium (Leinders-Zufall et al., 2000, 2004; He et al., 2008). Our concurrent recordings of calcium signals and extracellular electrical signals showed that calcium signals correlated with urine-evoked spiking activities in the VNO neurons (Fig. 2*C*). This was in agreement with a previous report (Leinders-Zufall et al., 2000). Thus, calcium imaging from G-CaMP2-expressing VNO neurons provided readout of pheromone activations. The system also allowed us to visualize large populations of neurons responding to various pheromone stimuli. Because of the mosaicism in transgene expression, G-CaMP2 was stochastically expressed in the neuronal population in the VNO. The stochastic expression pattern allows neurons expressing different receptors to be sampled. In the slice preparations, each slice was estimated to contain ~200–300 G-CaMP2-expressing cells. Urine at various concentrations evoked reproducible responses from 40–90 cells per slice, corresponding to ~25–35% of G-CaMP2-positive cells. A total of 557 cells from nine slices obtained from six animals (four males and two females) responded to different urine samples (supplemental Table 1, available at www.jneurosci.org as supplemental material). Ringer's control elicited little responses (supplemental Movies 1, 3, available at www.jneurosci.org as supplemental material) (see Fig. 4).

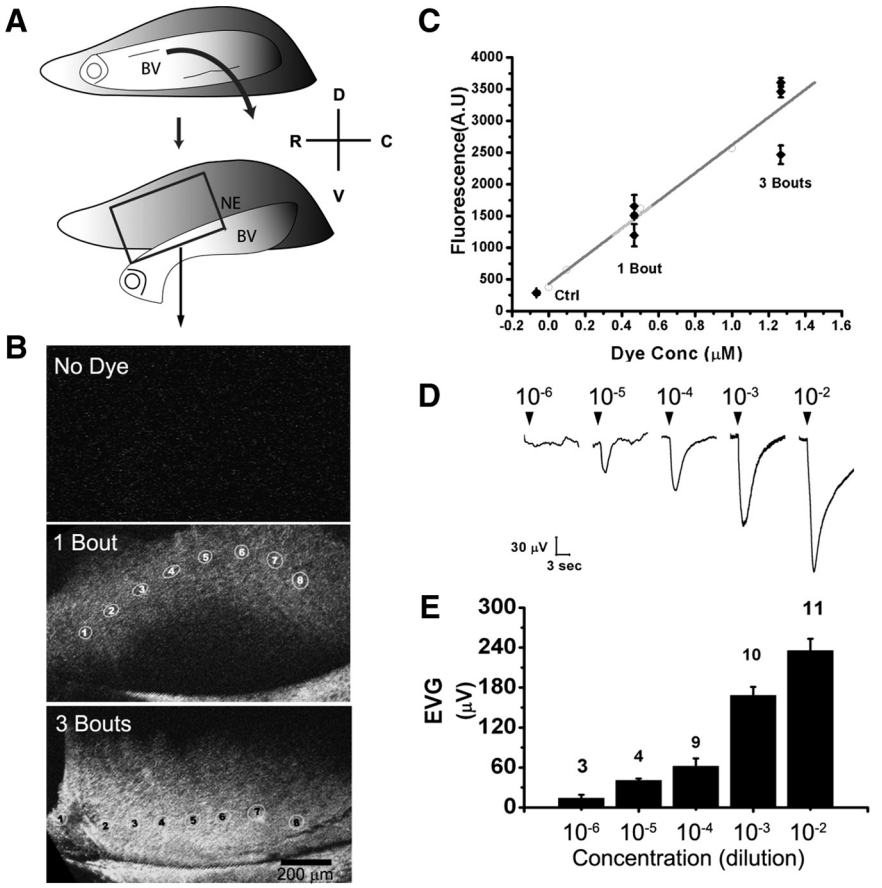

Figure 1. Effective concentrations of urine that activate the VNO. ***A***, Schematic diagram showing the surgical procedure to remove the blood vessel (BV) to expose the underlying neuroepithelium (NE). The orientation of VNO is marked as follows: D, dorsal; V, ventral; R, rostral; C, caudal. The rectangular frame indicates the area in which confocal imaging is performed, shown in ***B***. ***B***, Fluorescent images of dissected VNO from animals exposed to dye-labeled urine painted on the urogenital areas of anesthetized mice. The images are maximal projections of multiple *Z*-stacks obtained at different depths. The differences in curvature of the images reflect geometric variations in dissected VNO. Scale bar, 200 μm. ***C***, Quantification of fluorescent intensities in the VNO. Straight line is the standard curve derived from measurements from solutions containing dye at different concentrations (open circles). Measurements from six animals, three with one-bout investigation and three with three-bout investigations (filled diamonds) are plotted. Control (no dye) is also shown. For each animal, eight ROIs are measured, and the means ± SEM value are plotted. ***D***, EVG traces in response to 10^{-6} to 10^{-2} dilution of B6 male urine. Arrowheads indicate 1 s applications of diluted urine. ***E***, Bar graph showing averaged responses from multiple recordings. Numbers of recordings for each concentration are indicated above the bars. Data are represented as mean ± SEM.

When different dilutions of male and female mouse urine were applied, we observed different populations of cells being activated, and the responses to different dilutions were consistent across experiments using VNO slices from both male and female animals (nine slices from six animals) (Fig. 2*A*,*B*) (supplemental Table 1, available at www.jneurosci.org as supplemental material). In addition to changes in the response amplitude (Fig. 2*G*,*H*), we found a general increase in the number of activated cells by high-concentration urine from both male and female mice (Fig. 2*A*,*B*,*D*) (supplemental Table 1, available at www.jneurosci.org as supplemental material). Urine at 10^{-2} dilution elicited responses from approximately five times the number of cells as at 10^{-6} dilution ($n = 418$ at 10^{-2} and 81 at 10^{-6}). There was a slight difference between the change in the number of cells activated by male and female urine: male urine appeared to elicit a sharper increase in activated cells at 10^{-2} dilution (Fig. 2*D*). Urine further diluted to 10^{-8} elicited weak responses from very few cells (supplemental Fig. 4, available at www.jneurosci.org as supplemental material).

Detailed analyses of the responding neurons revealed a dynamic recruitment of different populations of cells at various concentrations. The profiles of cells activated by various concentrations of urine were distinct from one another (Fig. 2*E*,*F*) (supplemental Table 1, available at www.jneurosci.org as supplemental material). Quantitative analysis further revealed that individual cells also displayed different dose-dependent responses. Based on their concentration-dependent activation, we grouped the neurons into four broad categories. Type I cells were only activated by low but not high concentration of urine (Fig. 2*E–G*). They constituted ~9% of all responding cells ($n = 52$ of 557 total cells) (Fig. 2*I*). Type II cells displayed responses across all concentrations tested (Fig. 2*E–G*) and represented 2.7% ($n = 15$) of the cells. Type III cells were those activated by high concentrations of urine and represented the largest population (~69%; $n = 383$) of responding neurons (Fig.

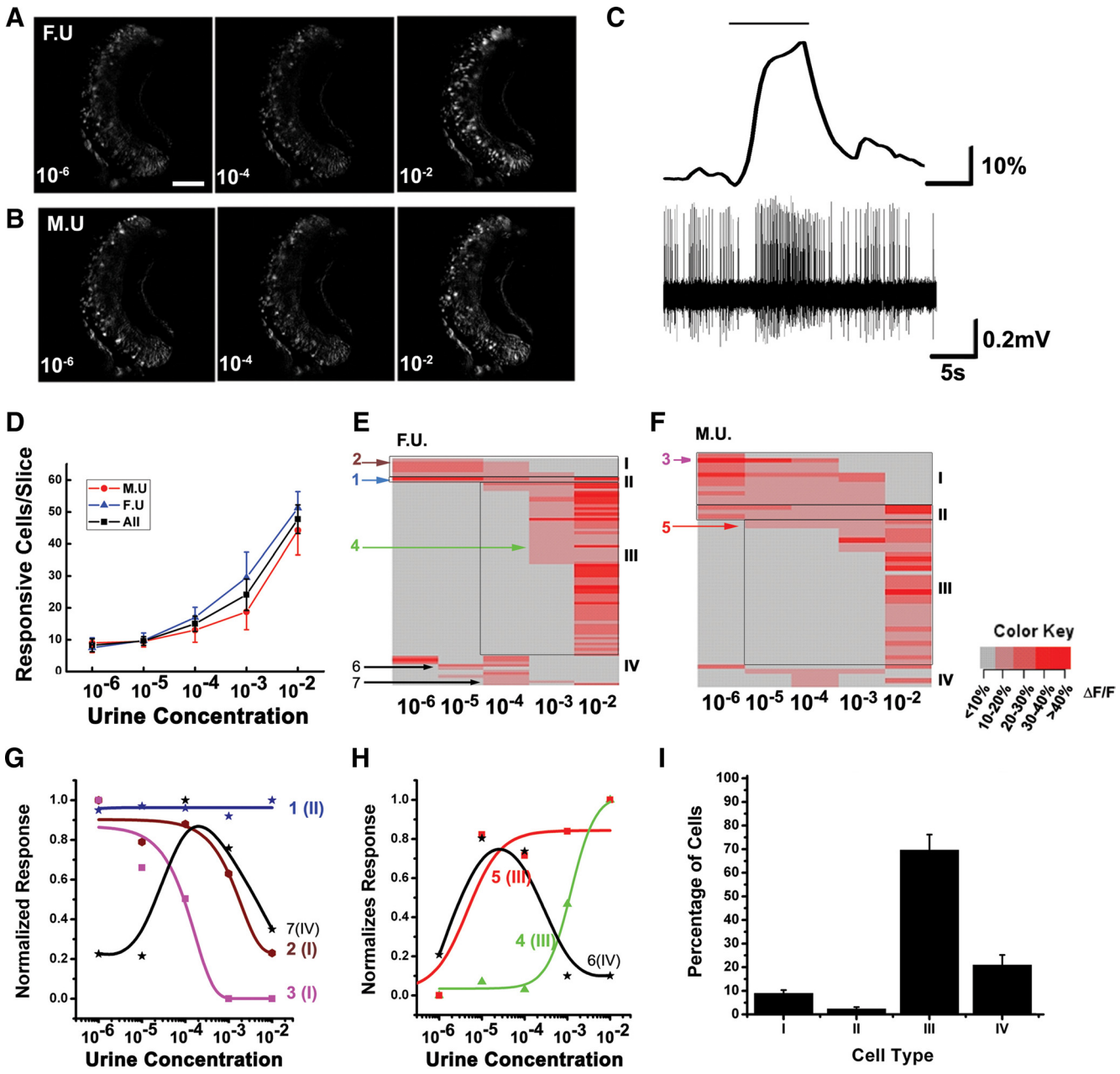

Figure 2. Dose-dependent response to mouse urine. ***A***, ***B***, Images of VNO neurons responding to male (M.U.) and female (F.U.) urine at various concentrations (10^{-6} to 10^{-2} dilutions). Scale bar, 100 μm. ***C***, Correspondence between calcium signal and electrical signal. Recordings from a G-CaMP2-expressing neuron in response to 1:100 female urine were shown. Urine triggered calcium signal (top) was simultaneously recorded with electrical responses (bottom). Black bar in the top indicates the duration of urine application. ***D***, Line graph shows increases in the number of responsive cells with increasing concentrations of urine for all urine samples (black square), male urine alone (red diamond), and female urine alone (blue triangle). ***E***, ***F***, Responses of individual cells to different concentration of urine are plotted as heat maps. The heat maps are based on the amplitude of individual responses. In this example, a total of 84 cells responded to female urine (***E***), and 50 cells responded to male urine (***F***). Different types of responses (types I–IV; see Results) are boxed and marked. ***G***, ***H***, Representative dose–response curves of individual neurons for type I, II, and IV (***G***) and type III and IV (***H***) cells. ***I***, Distribution of percentages of type I–IV cells for the overall responsive neuron population. Examples (***A***, ***B***, ***E–H***) are from animal 2 listed in supplemental Table 1 (available at www.jneurosci.org as supplemental material). Ensemble data (***D***, ***I***) are from total 557 responsive cells of nine slices and six animals (supplemental Table 1, available at www.jneurosci.org as supplemental material). Color key: 0, $\Delta F/F < 10\%$; 1, $10\% \leq \Delta F/F < 20\%$; 2, $20\% \leq \Delta F/F < 30\%$; 3, $30\% \leq \Delta F/F < 40\%$; 4, $\Delta F/F \geq 40\%$.

2*E*,*F*,*H*,*I*). Some of these cells showed canonical dose–response curves, i.e., increased urine concentrations elicited larger response amplitudes that plateaued at higher concentrations (Fig. 2*H*). Another group, the type IV cells (~19%; $n = 107$), showed atypical responses. Some of the type IV cells were activated by urine at both low and high concentrations but not at the intermediate ones, whereas others were activated by intermediate concentrations only (Fig. 2*E–I*).

The observation of the type I and type IV cells was surprising and had not been reported previously. In experiments with repeated applications of different urine samples, cells showed reproducible responses to the same stimuli at low or high con-

centrations of urine (supplemental Figs. 5, 6, available at www.jneurosci.org as supplemental material). A previous study of VNO response to natural stimuli with multielectrode recordings primarily revealed monotonic increase in response amplitude to increasing concentration of urine from 3×10^{-4} to 1/30 dilution of urine (Holy et al., 2000). This was primarily consistent with the type III cells, which constituted the majority of responding neurons and were activated at relatively high concentrations of urine ($>10^{-4}$ dilution). The type I cells were only revealed at the lower concentrations because they were likely obscured by high concentrations of urine (see below). Therefore, there is no significant contradiction in observations between the two studies.

Because of the presence of different types of cells, the identities of responding cells for low versus high concentrations were dramatically different. Most cells activated at 10^{-6} responded also to 10^{-5} and 10^{-4} dilutions (Fig. 2*E–G*, type I). Cells that were activated at 10^{-3} were mostly activated at 10^{-2} (Fig. 2*E*,*F*,*H*, type III). Only 2.7% of the responsive cells were shared by both low (10^{-6} to 10^{-4}) and high (10^{-3} to 10^{-2}) concentrations of urine (Figs. 2*A*,*B*,*F*,*G*, type II). The diminished response from one population of cells and the activation of another implied that the perception of the same urine at various concentrations were likely to be different.

Information conveyed by different concentrations of urine

We wondered whether the patterns of activity could reveal the nature of the signals. Our previous study has shown that urine contains cues to allow the discrimination of gender, strain, and individuals (He et al., 2008). In particular, we have found a very small set of neurons that uniquely identify the sex of an animal. The male urine-specific cells (MUSCs), responded to all male urine samples regardless of strain but not to any female urine and vice versa for the female urine-specific cells (FUSCs) (He et al., 2008). We performed similar analyses across different concentrations of urine samples by stimulating the VNO slices with urine from multiple individuals differing in strain and sex. These experiments were performed from an additional four slices from three animals (one male and two females). At high concentrations, these cells were readily identifiable, and the vast majority of MUSCs and FUSCs were activated at 10^{-2} dilution (Fig. 3*A–C*). The percentage of MUSCs and FUSCs dropped significantly at 10^{-3} dilution. At 10^{-2}, cluster analyses of the patterns of activation by multiple urine samples showed that they were segregated first according to sex and then according to strain, consistent with our previous report (Fig. 4*A*,*B*) (He et al., 2008). High

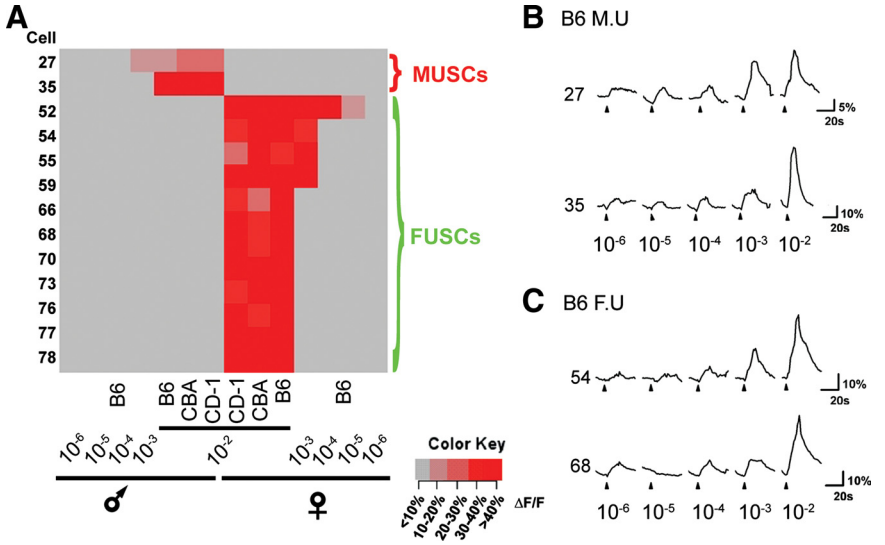

Figure 3. Dose-dependent activation of MUSCs and FUSCs. ***A***, Heat map of identified MUSCs and FUSCs in response to various concentrations of B6 male or female urine, as well as to 10^{-2} dilution of CBA and CD-1 male and female urine. ***B***, Response traces of two MUSCs to different concentrations of B6 male urine. ***C***, Response traces of two FUSCs to different concentrations of B6 female urine. Horizontal lines in ***B*** and ***C*** indicate background level activation. The results are obtained from a 6-month-old male and a 5-month-old female mouse.

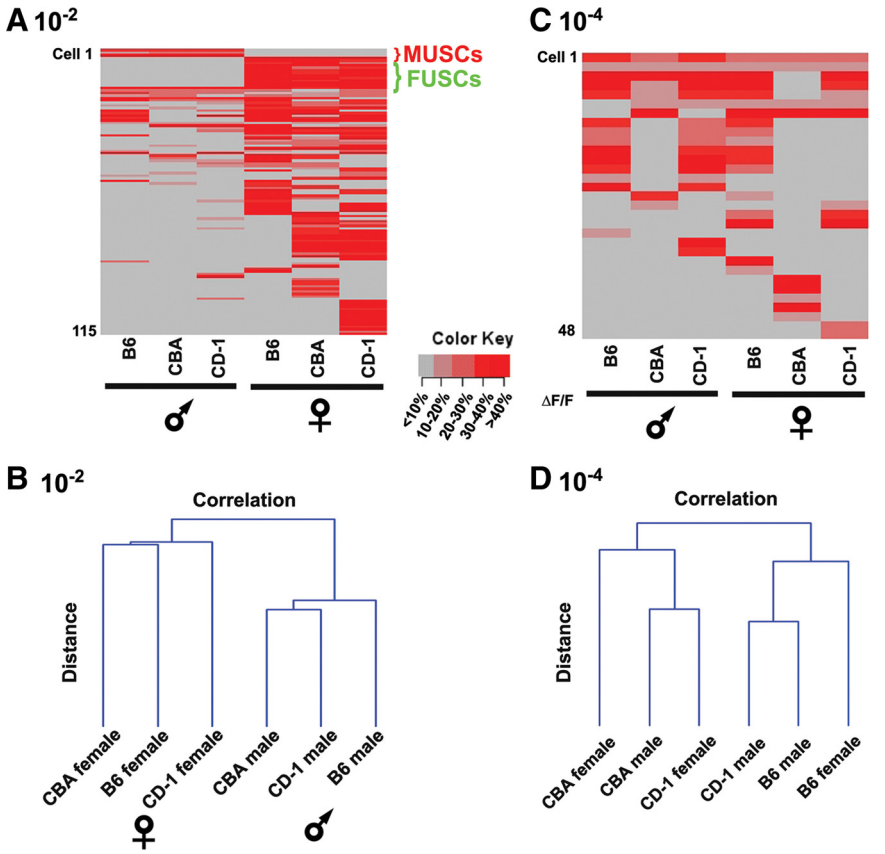

Figure 4. Dose-dependent activation of VNO neurons by individual urine samples. ***A***, Heat map of VNO neurons by 10^{-2} dilution of individual urines of different sex and strain. ***B***, Cluster analyses show grouping of urine samples according to sex at 10^{-2}. ***C***, Heat map of VNO neurons by 10^{-4} dilution of individual urines of different sex and strain. ***D***, Cluster analyses of urine samples indicate no apparent grouping at 10^{-4}. The results are from a 6-month-old female mouse.

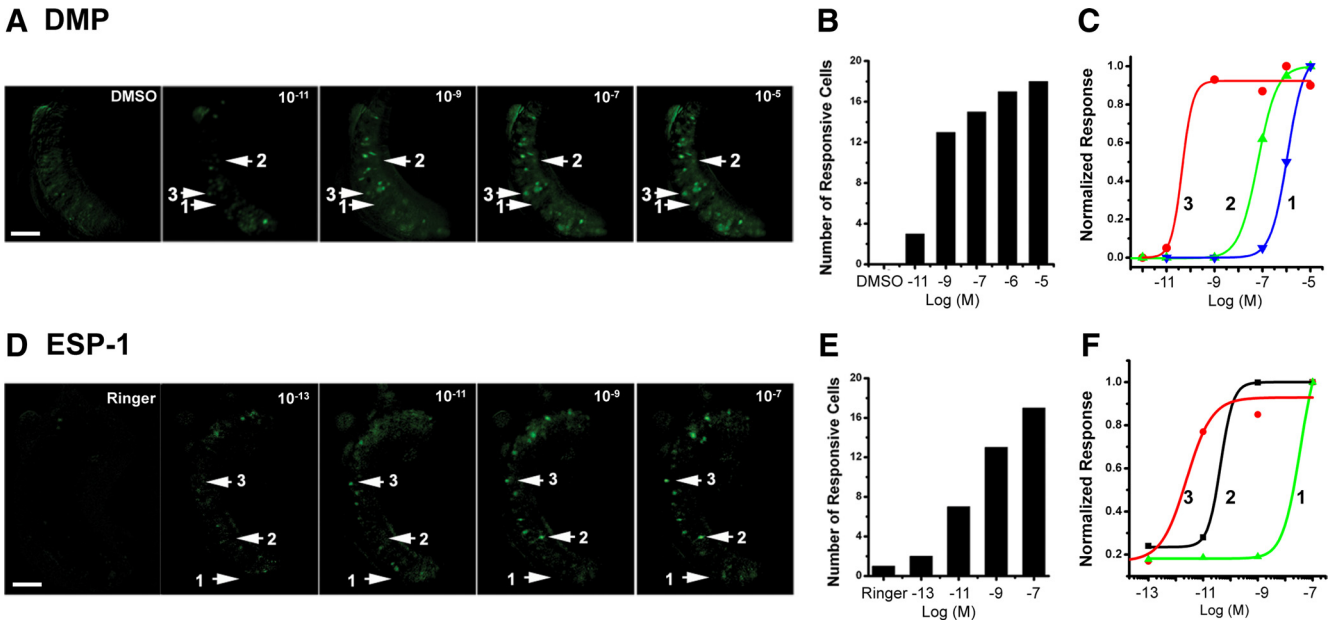

Figure 5. Dose-dependent responses single pheromones. ***A***, Images of VNO neurons responding to DMP at various concentrations (10^{-11} to 10^{-5} M, 0.1% DMSO solution as negative control). ***B***, Histogram shows an increase in the number of responsive neurons activated by increasing concentrations of DMP. ***C***, Examples of dose–response curves of different individual neurons indicated in ***A***. ***D***, Images of the VNO neurons responding to ESP-1 at various concentrations (10^{-13} to 10^{-7} M, Ringer's solution as negative control). ***E***, Histogram shows an increase in the number of responsive neurons activated by increasing concentrations of ESP-1. ***F***, Examples of dose–response curves of different individual neurons as indicated in ***D***. The results are from six animals (3 male and 3 female). Scale bars, 100 μm.

concentrations thus allowed the discrimination of individual urine samples according to the genders.

In contrast, low concentrations of urine-elicited responses from a smaller population of cells, none of which could be identified as MUSCs or FUSCs (Fig. 4*C*). At 10^{-4} dilution, the population of cells activated was similar to that activated by 10^{-5} and 10^{-6} dilutions (Fig. 2*E*,*F*). However, cluster analyses showed no pattern of segregation according to sex (Fig. 4*D*). Nevertheless, these patterns of activation were different for different strains and different individuals, suggesting that even at low concentration natural pheromones contain sufficient information to signal individual differences.

Response to single pheromone compounds

What is the mechanism underlying the dose-dependent activation of distinct cell populations? We wondered how well individual pheromone compounds could recapitulate the concentration-dependent activation by urine. The VNO expresses two large classes of pheromone receptors, the V1Rs and the V2Rs (Dulac and Axel, 1995; Herrada and Dulac, 1997; Matsunami and Buck, 1997; Ryba and Tirindelli, 1997). Low-molecular-weight organic compounds most likely activate the V1R family of receptors, whereas the V2Rs are likely to be activated by protein or peptide pheromones (Leinders-Zufall et al., 2000, 2004; Loconto et al., 2003; Kimoto et al., 2005). We therefore studied the dose-dependent activation of VNO neurons by synthetic compounds that included 2-heptanone, 2,5-dimethylpyrazine (DMP) and α- and β-farnesenes, sulfated steroid compounds (Jemiolo et al., 1986, 1989; Novotny et al., 1990; Nodari et al., 2008), as well as the ESP-1 and major histocompatibility complex peptides (Leinders-Zufall et al., 2004, 2009; Kimoto et al., 2005).

The urinary compounds were found to be present at micromolar concentrations in mouse urine (Novotny et al., 2007; Nodari et al., 2008). We therefore stimulated VNO slices with single compounds across a range of concentrations (10^{-13} to 10^{-5} M) that were likely to be encountered by the neurons in natural settings. Similar to urine, increased concentration of single compounds elicited responses from more cells (Fig. 5). For example, DMP, a presumed female pheromone, at 10^{-5} M activated approximately six times the number of cells of that at 10^{-11} M (Fig. 5*A*,*B*). The ESP-1 peptide, expressed in the male mice, activated approximately eight times the number of cells across six orders of concentrations (10^{-13} to 10^{-7} M) (Fig. 5*D*,*E*) (supplemental Movie 4, available at www.jneurosci.org as supplemental material). Detailed examination showed that different cells exhibited sigmoidal dose–response curves (Fig. 5*C*,*F*). These cells showed distinct sensitivities to the same chemicals, spanning four orders of magnitude. We analyzed >200 cells (from three male and three female animals) responding to single compounds and only found four cells showing nonconventional dose-dependent response.

Masking of type I cells

What is the mechanism responsible for the nonconventional dose-dependent activation of type I cells? In the main olfactory neurons, strong excitation can lead to temporary suppression of spikes attributable to inactivation of the voltage-gated channels (Duchamp-Viret et al., 2003; Rospars et al., 2008; Tan et al., 2010). The vomeronasal neurons, however, do not display this behavior. They fire nonadapting action potentials, and the responses show a generally positive correlation with stimulus intensity (Liman and Corey, 1996; Holy et al., 2000; Leinders-Zufall et al., 2000; Ukhanov et al., 2007; Nodari et al., 2008). Because of this property, it is unlikely that temporary spike suppression can underlie the unconventional responses. Nevertheless, we performed simultaneous electrophysiological recording and calcium imaging to examine the mechanism. Recording from a type I cell showed that a strong calcium response coincided with increased

spiking at low concentration of urine (10^{-5} dilution). The cell fired few spikes and showed little calcium response at higher concentrations (10^{-4} and 10^{-3} dilutions) (Fig. 6*A*). The calcium responses of the type III cell at high concentration of urine (10^{-2} dilution) also correlated with the spike responses (Fig. 2*C*).

Because individual putative pheromone components displayed conventional dose-dependent response, we reasoned that two likely mechanisms could explain the behavior of type I cells. The diminution in responses to high-concentration pheromones could be attributable to inactivation or desensitization. However, we observed little inactivation in single-compound experiments. Alternatively, these neurons could be actively suppressed by compounds in high-concentration urine. We tested these two hypotheses by examining the response of VNO neurons to different urine samples at different concentrations and their mixtures.

We first compared the activation patterns by individual urine samples at 10^{-4} and 10^{-2} dilution to that of the mixtures (Fig. 6*B*,*C*). Surprisingly, the patterns of activation by these mixtures were not simply the sum of the two samples. Patterns of activation elicited by mixtures generally conformed to that elicited by high-concentration urine. The activation by a mixture of 10^{-2} B6 male urine and 10^{-4} CD-1 male urine primarily recapitulated that of the 10^{-2} B6 male and vice versa (Fig. 6*B*). This was not simply attributable to the smaller number of cells activated by low-concentration urine. A number of cells that were activated at 10^{-4} dilution no longer responded to the mixture. With no exception, all cells responding to low but not high concentrations of urine failed to respond to a mixture if it contained high-concentration urine (Fig. 6*B*,*C*).

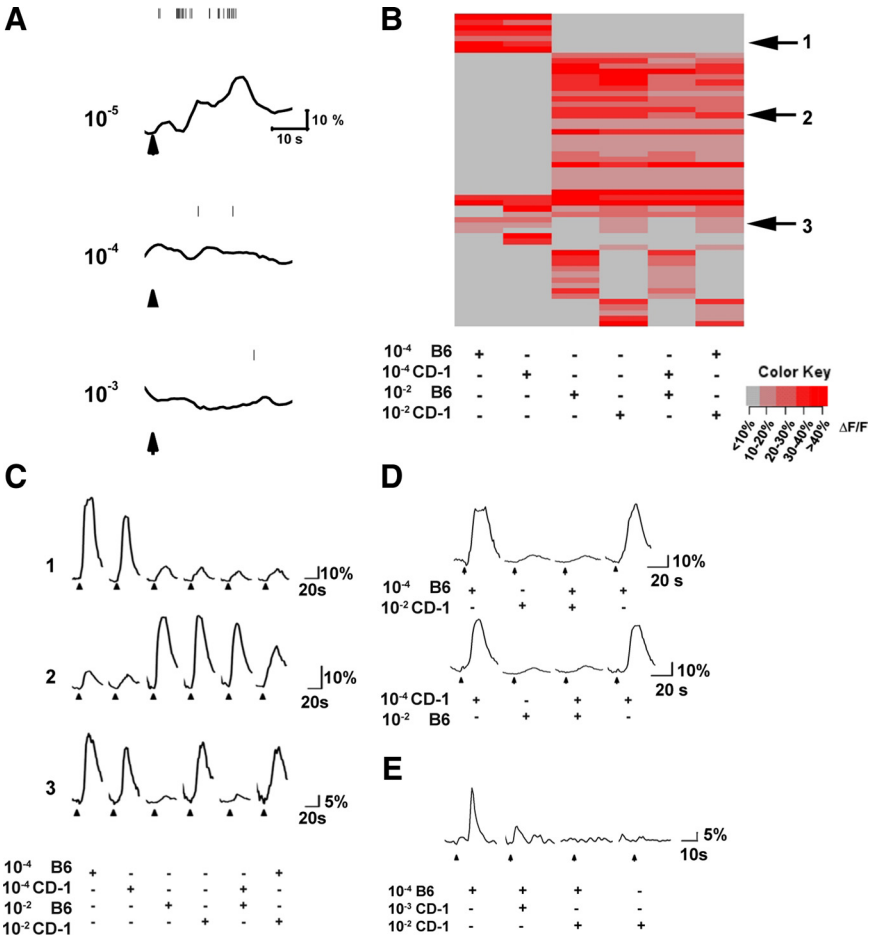

Figure 6. Masking of low-concentration urine by high-concentration urine in mixtures. ***A***, Simultaneous electrophysiological recording and calcium imaging from a type I cell in response to three different concentrations of urine. Vertical lines indicate individual spikes recorded from this cell. The traces indicate calcium signals. Arrows indicate the starting points of 5 s urine applications. The recordings were obtained from a slice prepared from a 6-month-old male mouse. ***B***, Heat map of activated VNO neurons by urine from two individual males at different concentrations. ***C***, Response traces for three cells indicated in ***B***. ***D***, Response traces for two cells that are activated by low-concentration urine. They are activated again immediately after application of high concentration of urine and mixture, which did not elicit any responses. ***E***, Response trace for a cell activated by low concentration of B6 urine but not high concentration of CD-1 urine. The responses to 10^{-4} B6 urine mixed with different concentrations of CD-1 urine are shown. The data are from a total of nine animals (5 male and 4 female; 2–5 months old), and examples shown here are from 3-month-old female mice.

To test the desensitization hypothesis, we next conducted experiments in which low-concentration urine was applied immediately after high-concentration urine or urine mixtures. If a cell responding to low-concentration urine was desensitized at high concentration, one would expect the subsequent application of low-concentration urine to elicit smaller or no responses. However, consecutive applications of urine at different concentrations showed little desensitization or inactivation (Fig. 6*D*). This was consistent with results from a set of experiments examining the response of VNO neurons to paired-pulse application of urine stimuli with various interpulse intervals. In these experiments, we observed little sign of inactivation, even with successions of applications with 10 s interpulse intervals (supplemental Fig. 5, available at www.jneurosci.org as supplemental material). In another example, the activation of a cell that responded to urine from a CD-1 male at both low (10^{-4}) and high (10^{-2}) concentrations, but not to urine from a B6 male at high concentration (10^{-2}), was suppressed by the mixture containing 10^{-2} B6 urine (Fig. 6*C*, cell 3). If desensitization was responsible for the loss of activation, we would have expected that the cell not respond to 10^{-2} CD-1 urine. Moreover, we observed that the masking was dose dependent. For example, we found that cells activated by 10^{-4} B6 but not 10^{-2} CD-1 urine responded to a mixture of 10^{-3} CD-1 and 10^{-4} B6 urine with intermediate amplitude (Fig. 6*E*). Together, these results suggested that the suppression of response at high concentrations was attributable to the presence of an inhibitor in concentrated urine. The effect is specific because we did not observe such masking effect among urine samples at high concentrations (supplemental Fig. 7, available at www.jneurosci.org as supplemental material). These observations further suggested that the neurons activated at the two urine concentrations were activated by different components in the urine. Because type IV cells are not homogeneous, we currently do not have the means to discern and study them. Nevertheless, their behavior may result from more complex interactions among the pheromones.

Discussion

In the natural environment, innate investigative behaviors result in the exposure of the VNO not only to different concentrations of pheromones but also to cues mixed from different individuals. Our studies reveal the complex concentration-dependent activation of the VNO. High-concentration pheromones activate more cells, most likely because of more pheromone cues reaching the activation threshold. Conversely, cells activated by low-concentration urine are masked by high-concentration ones. As a result, urine at low and high concentrations activates distinct subsets of cells, with an apparent transition between 10^{-4} and 10^{-3} dilutions. In a previous report, neurons responding differentially to male and female urine were observed across the concentrations tested (Holy et al., 2000). In our experiments, pairwise comparison of VNO activation by individual male or female urine samples indeed shows differential responses, even at low concentrations. However, at low concentrations, the MUSCs and FUSCs are not activated. In our previous study (He et al., 2008), we found that these two populations of neurons are essential for sex identification. Thus, the differential responses elicited by low concentrations of urine more likely reflect individual differences. Only during active investigations of the urogenital areas can high concentrations of urinary pheromones reach the VNO. At this level, urine can activate the MUSCs and FUSCs and provide unambiguous information that allows fine discrimination of individuals, sex, reproductive, and social status. Lower concentrations of pheromones appear inadequate to provide such information.

Strikingly, lower concentrations of urine activate subsets of cells that are distinct from those activated by high concentrations. Moreover, the activation of these cells appears to be suppressed by compounds that are effective in high-concentration urine. The masking effect implies that the neurons activated at different concentrations are likely to express different receptors and tuned to different pheromone molecules in the urine. Hence, the downstream neural circuits are likely to be activated differentially by different concentrations of urine and convey separate social signals. Perceptual masking is observed in many sensory systems but mostly results from central mechanisms that involve network interactions in the brain (Popper and Fay, 1992; Logothetis, 1998; Macknik and Livingstone, 1998; Macknik, 2006; Yost et al., 2008). Competitive inputs may result in the suppression of certain signals as in the case of binocular rivalry (Blake and Logothetis, 2002; Zeman, 2004; Tong et al., 2006). In other cases, selective attention may result in the suppression of certain inputs (Tse et al., 2005; Macknik et al., 2008). Perceptual masking in the olfactory system appears to be an exception, because some odors can directly mask the activation of the OSNs in the nose (Kurahashi et al., 1994; Duchamp-Viret et al., 2003; Rospars et al., 2008). This is likely attributable to the fact that direct binding of odorants to their receptors are required to activate the OSNs. Masking odorants may bind to the same binding pocket or to a different site to result in competitive or noncompetitive antagonism. However, such antagonistic masking has not been observed or proposed for pheromone detection, although suppression was observed in the accessory olfactory bulb (Hendrickson et al., 2008). Unlike the main olfactory neurons, which generally are more promiscuous in interacting with different odorants, pheromone-sensing neurons are highly selective (Buck, 2000; Leinders-Zufall et al., 2000; Wyatt, 2003). The selectivity presumably allows highly specific information to be conveyed among animals of the same species (Wyatt, 2003). Our observation that pheromones could mask each other thus offers insight into a novel means to control the information being transmitted among animals.

At this time, we do not know the precise nature of the signals conveyed by the low-concentration urine, nor do we know the behavioral implications of the suppression of these signals. Considering that pheromones deposited in urine markings are likely to reach the mouse VNO at lower concentrations, we speculate that cells activated at these concentrations could be used to obtain a snapshot of the presence of other animals in the surroundings. For example, both male and female mice countermark over urine deposits left by other mice (Rich and Hurst, 1998, 1999; Nevison et al., 2003; Hurst and Beynon, 2004; Brennan and Kendrick, 2006). The freshly deposited urine could serve to mask the marks left by other animals, and the masking of low-concentration pheromones may reduce the influence of unwanted signals. This is important for forming pheromone-related memory because the animals live in an environment laden with signals from many individuals. Additionally, volatile compounds in urine marks will get weaker over time, whereas peptides may get concentrated. The differential patterns evoked by marks at different ages can provide additional information of scent marks. In any case, behavioral experiments have shown complex interactions among different sources of pheromones. The presence of female pheromones could significantly dampen inter-male aggression, whereas male pheromones override signals from group-housed female in synchronizing estrus (Bronson, 1971). Urine from sexually experienced male can also suppress the effect of female urine in elevating luteinizing hormone levels in conspecific males (Clancy et al., 1988). Our results with urine mixtures suggest some antagonistic interactions at the receptor level, although computations within the neural circuitry in the brain could also occur.

References

Beauchamp GK, Martin IG, Wysocki CJ, Wellington JL (1982) Chemoinvestigatory and sexual behavior of male guinea pigs following vomeronasal organ removal. Physiol Behav 29:329–336.

Belluscio L, Koentges G, Axel R, Dulac C (1999) A map of pheromone receptor activation in the mammalian brain. Cell 97:209–220.

Beynon RJ, Hurst JL (2003) Multiple roles of major urinary proteins in the house mouse, *Mus domesticus*. Biochem Soc Trans 31:142–146.

Birch MC (1974) Pheromones. New York: American Elsevier.

Blake R, Logothetis NK (2002) Visual competition. Nat Rev Neurosci 3:13–21.

Brennan PA, Kendrick KM (2006) Mammalian social odours: attraction and individual recognition. Philos Trans R Soc Lond B Biol Sci 361:2061–2078.

Bronson FH (1971) Rodent pheromones. Biol Reprod 4:344–357.

Bronson FH (1979) The reproductive ecology of the house mouse. Q Rev Biol 54:265–299.

Buck LB (2000) The molecular architecture of odor and pheromone sensing in mammals. Cell 100:611–618.

Clancy AN, Singer AG, Macrides F, Bronson FH, Agosta WC (1988) Experiential and endocrine dependence of gonadotropin responses in male mice to conspecific urine. Biol Reprod 38:183–191.

Del Punta K, Puche A, Adams NC, Rodriguez I, Mombaerts P (2002) A divergent pattern of sensory axonal projections is rendered convergent by second-order neurons in the accessory olfactory bulb. Neuron 35:1057–1066.

Drickamer LC (1982) Delay and acceleration of puberty in female mice by urinary chemosignals from other females. Dev Psychobiol 15:433–445.

Drickamer LC (1986) Acceleration and delay of puberty in female mice via urinary chemosignals: age of the urine stimulus. Dev Psychobiol 19:155–161.

Drickamer LC, Assmann SM (1981) Acceleration and delay of puberty in female housemice: methods of delivery of the urinary stimulus. Dev Psychobiol 14:487–497.

Duchamp-Viret P, Duchamp A, Chaput MA (2003) Single olfactory sensory neurons simultaneously integrate the components of an odour mixture. Eur J Neurosci 18:2690–2696.

Dulac C, Axel R (1995) A novel family of genes encoding putative pheromone receptors in mammals. Cell 83:195–206.

He J, Ma L, Kim S, Nakai J, Yu CR (2008) Encoding gender and individual information in the mouse vomeronasal organ. Science 320:535–538.

Hendrickson RC, Krauthamer S, Essenberg JM, Holy TE (2008) Inhibition shapes sex selectivity in the mouse accessory olfactory bulb. J Neurosci 28:12523–12534.

Herrada G, Dulac C (1997) A novel family of putative pheromone receptors in mammals with a topographically organized and sexually dimorphic distribution. Cell 90:763–773.

Holy TE, Dulac C, Meister M (2000) Responses of vomeronasal neurons to natural stimuli. Science 289:1569–1572.

Humphries RE, Robertson DH, Beynon RJ, Hurst JL (1999) Unravelling the chemical basis of competitive scent marking in house mice. Anim Behav 58:1177–1190.

Hurst JL, Beynon RJ (2004) Scent wars: the chemobiology of competitive signalling in mice. Bioessays 26:1288–1298.

Jemiolo B, Harvey S, Novotny M (1986) Promotion of the Whitten effect in female mice by synthetic analogs of male urinary constituents. Proc Natl Acad Sci U S A 83:4576–4579.

Jemiolo B, Andreolini F, Xie TM, Wiesler D, Novotny M (1989) Puberty-affecting synthetic analogs of urinary chemosignals in the house mouse, *Mus domesticus*. Physiol Behav 46:293–298.

Johnston RE (1998) Pheromones, the vomeronasal system, and communication. From hormonal responses to individual recognition. Ann N Y Acad Sci 855:333–348.

Kaba H, Rosser A, Keverne B (1989) Neural basis of olfactory memory in the context of pregnancy block. Neuroscience 32:657–662.

Keverne EB (1998) Vomeronasal/accessory olfactory system and pheromonal recognition. Chem Senses 23:491–494.

Keverne EB (2002) Pheromones, vomeronasal function, and gender-specific behavior. Cell 108:735–738.

Kimoto H, Haga S, Sato K, Touhara K (2005) Sex-specific peptides from exocrine glands stimulate mouse vomeronasal sensory neurons. Nature 437:898–901.

Kurahashi T, Lowe G, Gold GH (1994) Suppression of odorant responses by odorants in olfactory receptor cells. Science 265:118–120.

Leinders-Zufall T, Lane AP, Puche AC, Ma W, Novotny MV, Shipley MT, Zufall F (2000) Ultrasensitive pheromone detection by mammalian vomeronasal neurons. Nature 405:792–796.

Leinders-Zufall T, Brennan P, Widmayer P, S PC, Maul-Pavicic A, Jäger M, Li XH, Breer H, Zufall F, Boehm T (2004) MHC class I peptides as chemosensory signals in the vomeronasal organ. Science 306:1033–1037.

Leinders-Zufall T, Ishii T, Mombaerts P, Zufall F, Boehm T (2009) Structural requirements for the activation of vomeronasal sensory neurons by MHC peptides. Nat Neurosci 12:1551–1558.

Leypold BG, Yu CR, Leinders-Zufall T, Kim MM, Zufall F, Axel R (2002) Altered sexual and social behaviors in trp2 mutant mice. Proc Natl Acad Sci U S A 99:6376–6381.

Liman ER, Corey DP (1996) Electrophysiological characterization of chemosensory neurons from the mouse vomeronasal organ. J Neurosci 16:4625–4637.

Loconto J, Papes F, Chang E, Stowers L, Jones EP, Takada T, Kumánovics A, Fischer Lindahl K, Dulac C (2003) Functional expression of murine V2R pheromone receptors involves selective association with the M10 and M1 families of MHC class Ib molecules. Cell 112:607–618.

Logothetis NK (1998) Single units and conscious vision. Philos Trans R Soc Lond B Biol Sci 353:1801–1818.

Macknik SL (2006) Visual masking approaches to visual awareness. Prog Brain Res 155:177–215.

Macknik SL, Livingstone MS (1998) Neuronal correlates of visibility and invisibility in the primate visual system. Nat Neurosci 1:144–149.

Macknik SL, King M, Randi J, Robbins A, Teller, Thompson J, Martinez-Conde S (2008) Attention and awareness in stage magic: turning tricks into research. Nat Rev Neurosci 9:871–879.

Matsunami H, Buck LB (1997) A multigene family encoding a diverse array of putative pheromone receptors in mammals. Cell 90:775–784.

Meister M, Bonhoeffer T (2001) Tuning and topography in an odor map on the rat olfactory bulb. J Neurosci 21:1351–1360.

Meredith M, O'Connell RJ (1979) Efferent control of stimulus access to the hamster vomeronasal organ. J Physiol 286:301–316.

Meredith M, Marques DM, O'Connell RO, Stern FL (1980) Vomeronasal pump: significance for male hamster sexual behavior. Science 207:1224–1226.

Mori K, Nagao H, Yoshihara Y (1999) The olfactory bulb: coding and processing of odor molecule information. Science 286:711–715.

Nevison CM, Armstrong S, Beynon RJ, Humphries RE, Hurst JL (2003) The ownership signature in mouse scent marks is involatile. Proc Biol Sci 270:1957–1963.

Nodari F, Hsu FF, Fu X, Holekamp TF, Kao LF, Turk J, Holy TE (2008) Sulfated steroids as natural ligands of mouse pheromone-sensing neurons. J Neurosci 28:6407–6418.

Novotny M, Schwende FJ, Wiesler D, Jorgenson JW, Carmack M (1984) Identification of a testosterone-dependent unique volatile constituent of male mouse urine: 7-exo-ethyl-5-methyl-6,8-dioxabicyclo[3.2.1]-3-octene. Experientia 40:217–219.

Novotny M, Harvey S, Jemiolo B, Alberts J (1985) Synthetic pheromones that promote inter-male aggression in mice. Proc Natl Acad Sci U S A 82:2059–2061.

Novotny M, Harvey S, Jemiolo B (1990) Chemistry of male dominance in the house mouse, *Mus domesticus*. Experientia 46:109–113.

Novotny MV, Ma W, Wiesler D, Zídek L (1999) Positive identification of the puberty-accelerating pheromone of the house mouse: the volatile ligands associating with the major urinary protein. Proc Biol Sci 266:2017–2022.

Novotny MV, Soini HA, Koyama S, Wiesler D, Bruce KE, Penn DJ (2007) Chemical identification of MHC-influenced volatile compounds in mouse urine. I. Quantitative proportions of major chemosignals. J Chem Ecol 33:417–434.

Pankevich D, Baum MJ, Cherry JA (2003) Removal of the superior cervical ganglia fails to block Fos induction in the accessory olfactory system of male mice after exposure to female odors. Neurosci Lett 345:13–16.

Pantages E, Dulac C (2000) A novel family of candidate pheromone receptors in mammals. Neuron 28:835–845.

Popper AN, Fay RR (1992) The mammalian auditory pathway: neurophysiology. New York: Springer.

Price MA, Vandenbergh JG (1992) Analysis of puberty-accelerating pheromones. J Exp Zool 264:42–45.

Ralls K (1971) Mammalian scent marking. Science 171:443–449.

Rich TJ, Hurst JL (1998) Scent marks as reliable signals of the competitive ability of mates. Anim Behav 56:727–735.

Rich TJ, Hurst JL (1999) The competing countermarks hypothesis: reliable assessment of competitive ability by potential mates. Anim Behav 58:1027–1037.

Rodriguez I, Feinstein P, Mombaerts P (1999) Variable patterns of axonal projections of sensory neurons in the mouse vomeronasal system. Cell 97:199–208.

Rospars JP, Lansky P, Chaput M, Duchamp-Viret P (2008) Competitive and noncompetitive odorant interactions in the early neural coding of odorant mixtures. J Neurosci 28:2659–2666.

Rubin BD, Katz LC (1999) Optical imaging of odorant representations in the mammalian olfactory bulb. Neuron 23:499–511.

Ryba NJ, Tirindelli R (1997) A new multigene family of putative pheromone receptors. Neuron 19:371–379.

Spehr M, Kelliher KR, Li XH, Boehm T, Leinders-Zufall T, Zufall F (2006) Essential role of the main olfactory system in social recognition of major histocompatibility complex peptide ligands. J Neurosci 26:1961–1970.

Tan J, Savigner A, Ma M, Luo M (2010) Odor information processing by the olfactory bulb analyzed in gene-targeted mice. Neuron 65:912–926.

Tong F, Meng M, Blake R (2006) Neural bases of binocular rivalry. Trends Cogn Sci 10:502–511.

Tse PU, Martinez-Conde S, Schlegel AA, Macknik SL (2005) Visibility, visual awareness, and visual masking of simple unattended targets are confined to areas in the occipital cortex beyond human V1/V2. Proc Natl Acad Sci U S A 102:17178–17183.

Ukhanov K, Leinders-Zufall T, Zufall F (2007) Patch-clamp analysis of gene-targeted vomeronasal neurons expressing a defined V1r or V2r receptor: ionic mechanisms underlying persistent firing. J Neurophysiol 98:2357–2369.

Wagner S, Gresser AL, Torello AT, Dulac C (2006) A multireceptor genetic approach uncovers an ordered integration of VNO sensory inputs in the accessory olfactory bulb. Neuron 50:697–709.

Wyatt TD (2003) Pheromones and animal behaviour: communication by smell and taste. Cambridge, UK: Cambridge UP.

Wysocki CJ, Lepri JJ (1991) Consequences of removing the vomeronasal organ. J Steroid Biochem Mol Biol 39:661–669.

Wysocki CJ, Wellington JL, Beauchamp GK (1980) Access of urinary nonvolatiles to the mammalian vomeronasal organ. Science 207:781–783.

Yang H, Shi P, Zhang YP, Zhang J (2005) Composition and evolution of the V2r vomeronasal receptor gene repertoire in mice and rats. Genomics 86:306–315.

Yost WA, Popper AN, Fay RR (2008) Auditory perception of sound sources. New York: Springer.

Yu CR, Power J, Barnea G, O'Donnell S, Brown HE, Osborne J, Axel R, Gogos JA (2004) Spontaneous neural activity is required for the establishment and maintenance of the olfactory sensory map. Neuron 42:553–566.

Zeman A (2004) Theories of visual awareness. Prog Brain Res 144:321–329.

Zhang X, Rodriguez I, Mombaerts P, Firestein S (2004) Odorant and vomeronasal receptor genes in two mouse genome assemblies. Genomics 83:802–811.